2020

Verification of the Vertical Bubble Flow Experiments

reginald jones ii
Virginia Commonwealth University

VERIFICATION OF THE VERTICAL BUBBLE FLOW EXPERIMENTS

A Thesis

Presented in Partial Fulfillment of the Requirements for the

Degree of Master of Science

with a

Major in Mechanical and Nuclear Engineering

in the

Graduate School

Virginia Commonwealth University

By

Reginald Jones

Major Professor: Supathorn Phongikaroon

July 2020

Mechanical and Nuclear Engineering

Virginia Commonwealth University

This is to certify that the dissertation prepared by Reginald Jones entitled "Verification of the Vertical Bubble Flow Experiments" has been approved by his committee as satisfactory completion of the dissertation requirement for the degree of <u>Master of Science</u>.

1

ABSTRACT

Detailed experimental design to support basic pedagogy of flow regimes – single phase liquid, bubbly, slug, annular, dispersed droplet, and single phase vapor – occurring in flow channels of nuclear reactors has been developed for EGMN 203 - Nuclear Engineering Practicum offering at Virginia Commonwealth University's Department of Mechanical and Nuclear Engineering. The laboratory instruction will be used to help students forming ideas and understanding flow regimes occurring in nuclear engineering applications. We designed and constructed four water columns to act as surrogates for water channels in a nuclear reactor. Each column was used for a different experiment: salted versus unsalted water, slug flow, and high-speed flow. Compressed air was injected into each system in order to demonstrate these concepts. Students would form a group and record data and photos for different experimental schemes. Preliminary results indicate that it is possible to adequately demonstrate bubbly, slug, plug and churn flow using the designed set up as well as photograph them using cell phone cameras. It is also possible to measure bubble velocities and diameters, as well as estimate bubble population using the provided method through ImageJ software. Churn flow is present in multiple conditions: as a constant flow pattern when air is injected into the system at a specific air pressure, as well as being a secondary flow pattern following the sudden injection of air to produce both slug and plug flows. In the slug and plug flow patterns, this churn flow dissipated upon the air pocket collapse. Both slug and plug flows were produced and volumes were easily able to be estimated using the water level pre-injection and the maximum displaced water height before the eventual pocket collapse, with slug flow water displacements of approximately 4.25" and plug flow water displacements as large as 7" being recorded.

ACKNOWLEDGEMENTS

I would first like to thank Dr. Supy for believing in me and seeing potential that I did not think I had, for always pushing me to be better because you knew I could do it. I would like to thank Professors Miller, Supy, and Goddard for making nuclear engineering interesting. Without the interest you three generated, I might have walked a different path in college. I would also like to thank Professor Milos and Professor Miller for being on my defense committee.

I would like to thank my fellow group members Dalsung, Dimitris, Michael, Adam, Hunter, George, and Riyadh for the encouragement to work through stressful times while also showing me how to be a better researcher and for being there to listen to any problem and offering advice.

Finally, I would like to thank my friends and my family for all of their support never questioning my decision to enter graduate school. Thank you for being there to push me through any hardships I faced.

TABLE OF CONTENTS

LIST OF FIGURES

7

LIST OF TABLES

ABBREVIATIONS AND NOMENCLATURE

AGR	Advanced gas reactor
BWR	Boiling water reactor
ΔT	Delta T,
FBR	Fast breeder reactor
fps	Frames per second
ft^3/h	Cubic feet per hour
g	gram
in^2	Inches squared
kPa	Kilo pascal
L	Liter
LWGR	Light water graphite moderated reactor
LWR	Light water reactor
m^3/h	Cubic meters per hour
min	Minute
mm	Millimeter
NaCl	Sodium chloride
PHWR	Pressurized heavy water reactor
ppi	Pixel per inch
psi	Pounds per square inch
PVC	Polyvinyl chloride (plastic)
PWR	Pressurized water reactor
q"	Heat flux
scfm	Standard cubic feet per minute
TA	Teaching assistant
T_s	Surface temperature
T_{sat}	Saturated temperature
UO_2	Uranium dioxide
W/m^2	Watts per meter squared

Chapter 1 Introduction

1.1. Background

A nuclear reactor can be utilized to convert energy released from nuclear fission into electricity through thermal hydraulics conceptual design. From this aspect, the energy from a nuclear chain reaction heats up the fuel in the core of the reactor and the coolant system carries this heat away. This heat can be used to boil water and the steam from this in turn is used to spin turbines. This process is similar to how coal and gas power plants operate, with the heat produced from burning those fuels is then used to boil water, which turns a turbine that provides the electricity. Here, the nuclear reactor is housed inside a pressure vessel.

Nuclear reactor fuel is usually UO_2 (uranium oxide), which is enriched to a set percentage, between 3 and 5% depending on reactor type, but never more than 19.9%. This fuel is in the shape of pellets that are fit into fuel rods. These rods are then gathered into a bundle known as a fuel assembly. Each assembly consists of hundreds of these rods and each reactor contains hundreds of these assemblies. These assemblies are placed in a roughly cylindrical shape and this forms the reactor core. A fuel assembly can be seen in Figure 1.1.
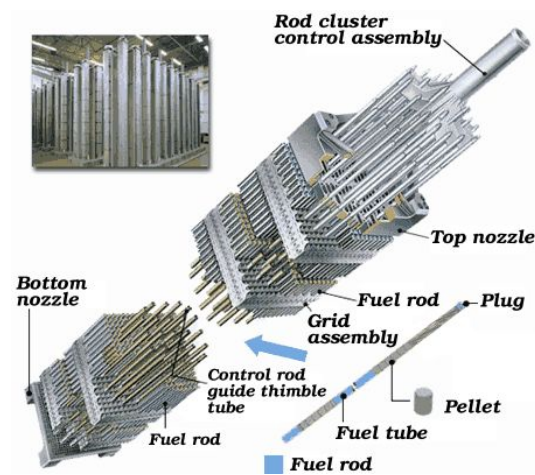
Figure 1.1: PWR Fuel Assembly [1]

The coolant in a nuclear reactor is used to pull heat away from the core and transfer it into water to make steam. This coolant may itself be water, but may also be liquid metals, molten salts, or a gas. There may be one or multiple coolant loops in a reactor. Nuclear reactors need be kept in control to prevent the reaction from getting out of hand. This can be accomplished by using control rods, which are made of boron or some other material that absorbs neutrons and enable the reactor operator to control the power coming out of the reactor. They are even able to stop a nuclear reaction in its tracks. Figure 1.2 is a diagram of a core, which includes the control rods, the spacer grids, and the fuel assemblies.
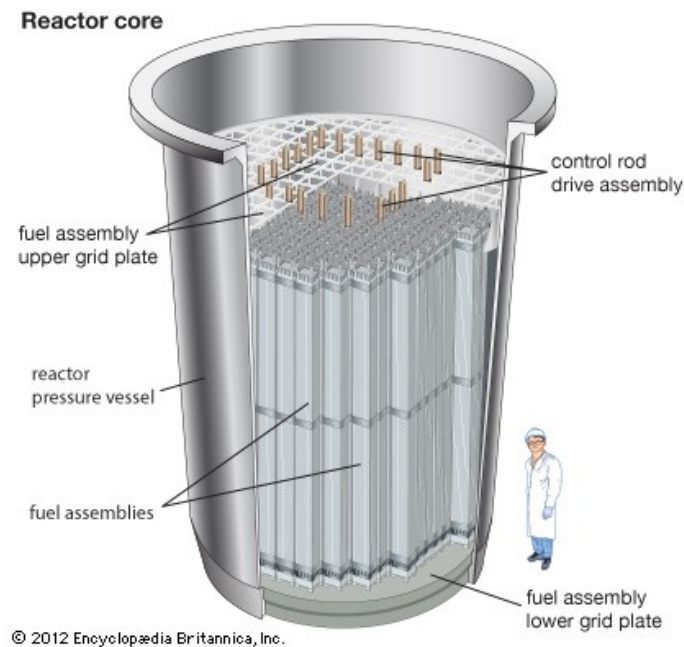
Figure 1.2: Reactor Core [2]

Reactor Types

There are different reactor types. This includes a light water reactor (LWR)—composing of a pressurized water reactor (PWR) and a boiling water reactor (BWR), the advanced gas-cooled reactor (AGR), the pressurized heavy water reactor (PHWR), the light water graphite-moderated reactor (LWGR), and the fast breeder reactor (FBR). The two that will briefly be discussed next are the BWR and PWR as these relate to the experimental design.

BWR

The BWR is a reactor in which water is boiled in the core. This water is boiled into steam in the upper part of the core as shown in Figure 1.3. The steam is then passed through the loop and to the turbines. Since this water comes into direct contact with the core, the turbine needs to be in some way protected from radiation and people who come in contact during maintenance must also wear protection. BWRs have fuel assemblies containing between 90-100 fuel rods, and there are up to 750 assemblies in a reactor core [3].
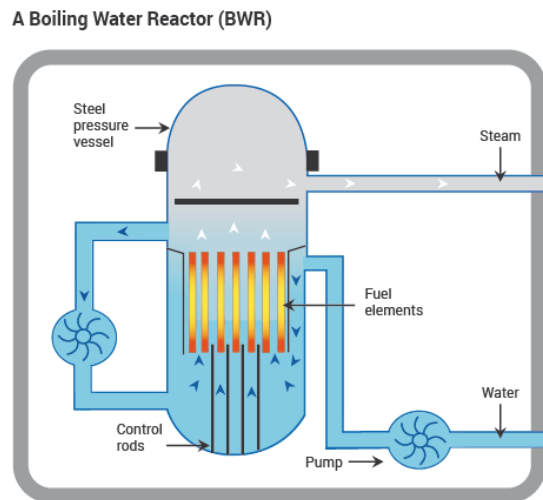
Figure 1.3: BWR Diagram [3]

PWR

The PWR is the most common reactor, with about 300 operable reactors for power generation and several hundred more employed for naval propulsion [3]. PWRs use water as the coolant and the

moderator. The coolant in a PWR is kept under high pressure in order to keep it in the liquid state, hence the name. This reactor has a secondary coolant loop used to create the steam for the turbine. PWRs have fuel assemblies of between 150 and 200 fuel rods and each core has between 200 and 300 assemblies [3]. Figure 1.4 shows a diagram of a PWR reactor.
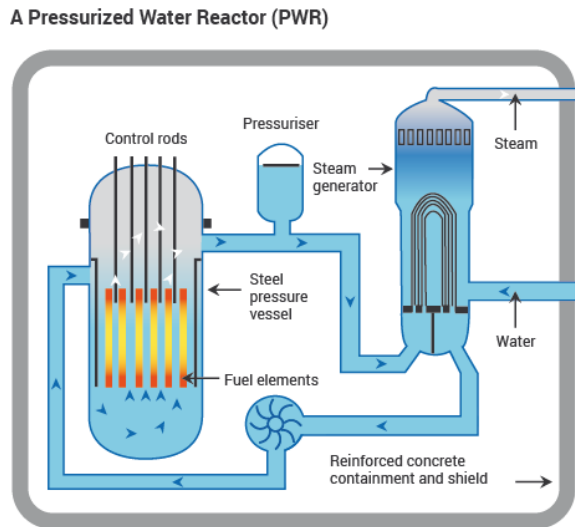
Figure 1.4: PWR Diagram [3]

In LWRs, the liquid water coolant enters through the bottom of a core. While flowing through the upwards through the core, this water absorbs and carries away the heat caused by fission reactions in the nuclear fuel. Figure 1.5 shows this, with water coolant flowing upwards and the heat radiating outwards (radially) from the nuclear fuel being absorbed being demonstrated by changing from dark to light blue; it is important to note that this color change is just for illustrative purposes.

13
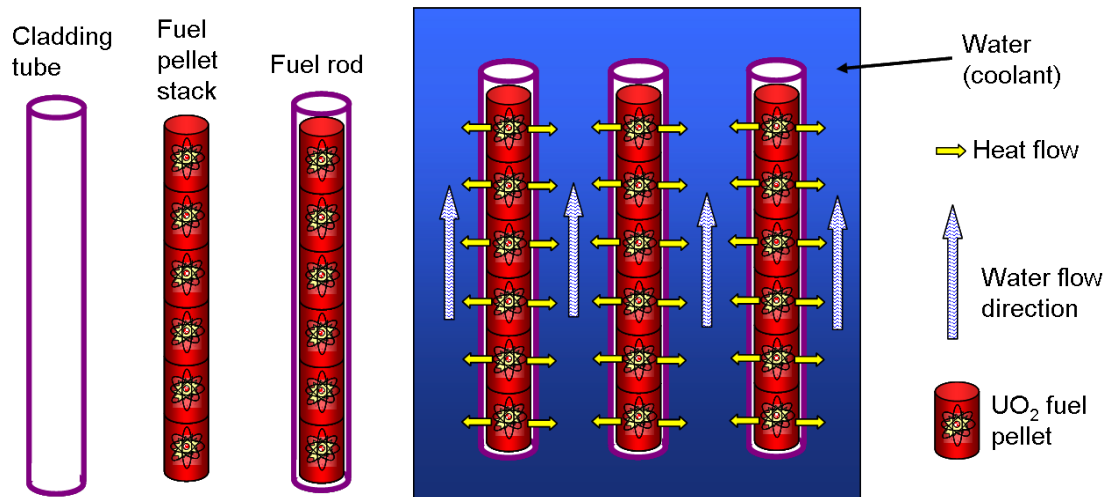
Figure 1.5: Schematic of reactor core heat flow from the nuclear fuel to the coolant

1.2. Basic Theory

1.2.1. Heat Transfer and Pool Boiling

In order to understand why we are simulating boiling we must first discuss conductive heat transfer. Conductive heat transfer occurs when heat is exchanged between different locations by a moving fluid; for example, the heat from a reactor core is being drawn away with the coolant to boil water for steam. The amount of heat (energy) transferred from the core to the coolant (water) is known as the heat flux, q", and is a measure of the energy per unit time (or power) transferred per unit of heat surface area. Figure 1.6 is a representation of pool boiling. Pool boiling occurs when the heated surface (reactor core) is submerged in an initially stagnant liquid (water). Heat flux is plotted on the y-axis of this diagram in units of W/m^2.

14
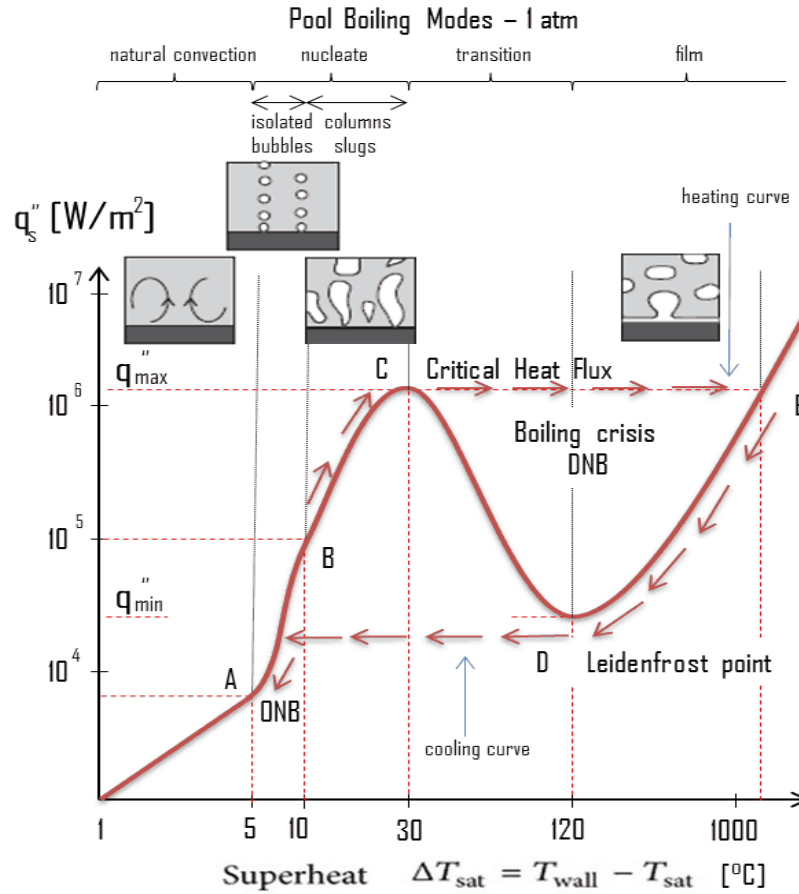
Figure 1.6: Pool Boiling [4]

The curve that starts at the origin and ends at point A of this figure represents the pool boiling mode known as natural convection boiling. When the object heats up, heat transfer takes place between the heater surface and water due to free or natural convection (this is similar to the heat flow from a nuclear fuel rod surface to the coolant). Natural convection occurs when the fluid movement is not caused by an outside source, such as a pump or fan. In this region, the heat flux and ΔT values start to increase. ΔT is the difference between the surface temperature (T_s) of the wall (fuel rod) and the saturation temperature (T_{sat}) of the coolant (water). Boiling occurs when the temperature of the coolant reaches its saturation temperature. Below this value the water is said to be 'subcooled.'

Curve AC represents the nucleate boiling mode. In this region, bubbles are formed at the bottom of the tank and start to rise. In the region shown by curve AB, the bubbles are isolated and eventually collapse. These bubbles increase the heat flux from surface to coolant and the coolant temperature increases. In the region shown by curve BC, the heat flux again rises and the bubbles move faster. These bubbles coalesce together forming slugs which rise through the liquid and at the top of the liquid break and the gases/vapor contained within are released. This region, AC, is what is to be explored and simulated in this lab.
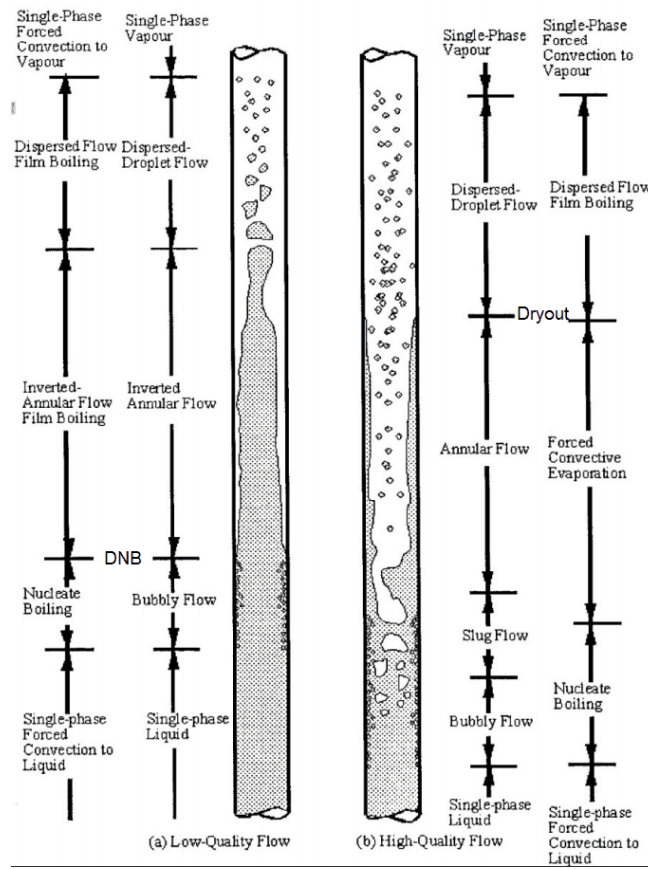
Figure 1.7: Regions of heat transfer in convective boiling in a flow channel with uniform wall heat flux are shown for both low-quality and high-quality flow [4].

1.2.2. Flow Patterns

There are various fluid flow patterns that can take place in these flow channels. For example, the flow patterns caused by the boiling behavior in a tubular flow channel as shown in Figure 1.7 above. On side (b) in this figure, there are see six main flow patterns: single phase liquid, bubbly, slug, annular, dispersed droplet, and single-phase vapor [5, 6].

o Bubbly Flow, depicted in Figures 8(a) and 8(b), occurs when a light fluid travels through a heavy fluid in bubbles (for example, steam bubbles through water). These bubbles are usually evenly distributed throughout.

o Slug flow, depicted in Figure 1.8(c), occurs in a system when the light fluid (steam) becomes trapped in large bubbles inside the heavier fluid (water). These bubbles are larger and move faster than those in plug flow and because of this, these bubbles tend to move the heavy fluid along their path. These bubbles are irregularly distributed.

o Churn flow, depicted in Figure 1.8(d), occurs when the large, fast moving slugs move up the center of the fluid filled channel. These slugs, generally containing a lighter fluid, end up pushing the heavy fluid to the channel walls. These slugs may regularly deform and, at high enough speeds, cause the churn flow to become annular flow.

o Annular flow, depicted in Figure 1.8(f), occurs when the light fluid flows through the channel center while the heavy fluid flows along the channel walls. This requires the inner lighter fluid to be traveling very quickly through the channel.

o Mist Flow/Dispersed Droplet Flow occurs when the lighter fluid velocity gets high enough that it carries small amounts of the heavy fluid with it as droplets. This is different than annular flow because there is not likely to be any of the heavy fluid along the channel walls.

- o <u>Plug flow</u> occurs in when large gas bubbles move around in a liquid. These bubbles make occupy much of the space inside a channel. These bubbles are smaller and move slower in comparison to those found in slug flow.
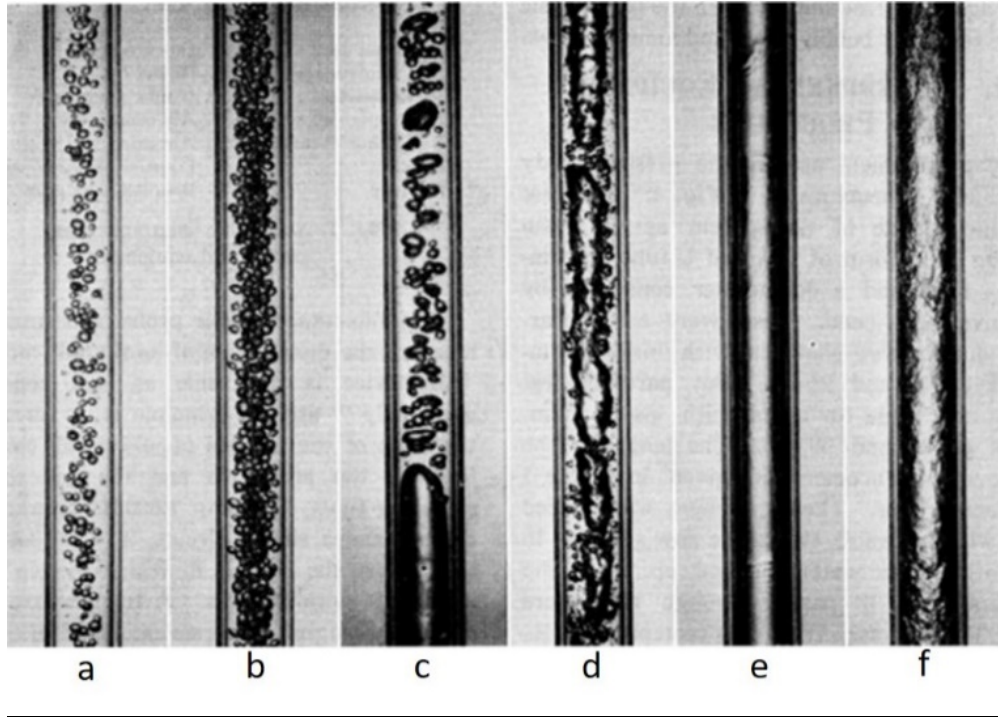
Figure 1.8: Flow Regimes: a. Bubbly; b. Bubbly; c. Slug; d. Churn; e. Film Drop; and f. Annular. [6]

1.3. Motivation, Goal, and Approach

Currently, there is no detailed experimental design to support basic pedagogy of flow regime for freshman nuclear engineering curriculum. This lack of information becomes the motivation to develop laboratory design demonstrating some basic principles of bubbly flow in a channel for EGMN 203 - Nuclear Engineering Practicum offering at Virginia Commonwealth University's Department of Mechanical and Nuclear Engineering. The laboratory instruction will be used to help students forming ideas and understanding flow regimes occurring in nuclear engineering applications. We developed and built four water columns to act as surrogates for water channels in a nuclear reactor. Each column was used for a different experiment: salted versus

unsalted water, slug flow, and high-speed flow. Compressed air was injected into each system in order to demonstrate these concepts. Students would form a group and record data and photos for different experimental schemes.

1.4 Dissertation Layout

Chapter 1 of this dissertation contains the goal and motivation of this dissertation along with background information. Chapter 2 provides information about the experimental set up, the conditions and procedures for analysis. Chapter 3 contains the preliminary results and discussion. Chapter 4 of this dissertation offers the summary and future recommendations.

Chapter 2 Experimental Setup

2.1. Equipment and Design

The water tanks used in the experiment were designed, built and assembled in-house using parts purchasing through McMaster Carr and Amazon. These items were cut in the VCU Innovation Center in the Department of Mechanical and Nuclear Engineering and retrofit in Molten Salt Group's laboratory area on the 1st floor of the East Engineering Building. A complete assembled tank is shown in Figure 2.1.
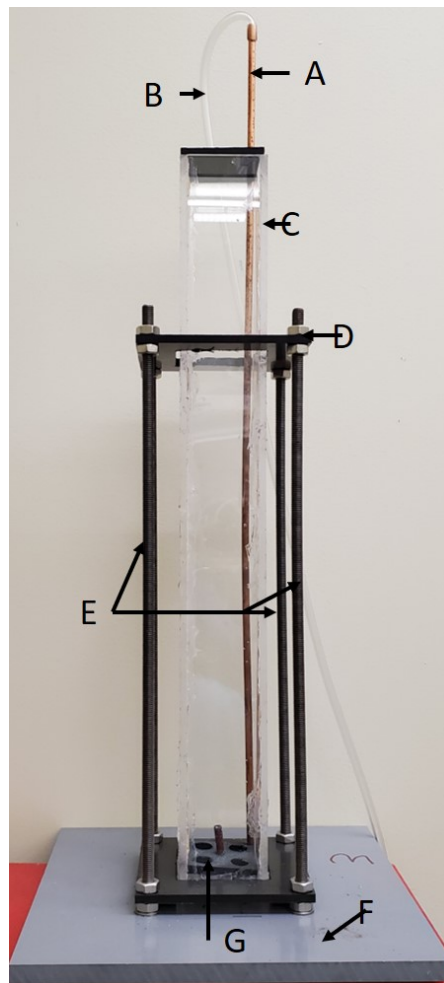
Figure 2.1: A full tank assembly: A is the copper tube, B is the rubber tube; C is the Plexiglas chamber; D is the PVC upper support; E are the threaded steel support rods; F is the PVC base; G is the lower copper tube support

Here, each tank consists of a copper tube, ordered from Grainger and point A in Fig (1), with diameters of 3/16, 3/8, and ½". Each tube was ordered at 6 feet and cut down to approximately 3 feet, and the ends were bent into a U with a turn radius of approximately 1 inch. This U bend is shown in closer detail in Figure 2.2. At the both ends of the copper tubing was a rubber tube, diameter of ¼" (McMaster Carr) and shown at point B in Figure 2.1. Attached to the submerged end of each copper tube was a 1" piece of the rubber tube and an air stone (1.2" Pawfly air stone—Model: ASR-030 with flow rate 1 L/min and required pump power of 2-4 W) purchased through Amazon (see Figure 2.3).

Figure 2.2: U bend in copper tube

Figure 2.3: Pawfly air stone installed in the tank

21

Each tank, shown at point C in Figure 2.1, was made from 7/32" Plexiglas (McMaster Carr) and machined in the Innovation lab. Points D and G, as well as the lid, were made from 1/4" black PVC (McMaster Carr). They were cut into the desirable shape in the Innovation Lab and finished in house. The threaded rods, 0.39" in diameter and connecting the supports to the base (see point E); these items were ordered from McMaster Carr. Point F, the base, was made from 1/2" high strength PVC (McMaster Carr) and machined in the lab. The compressed air tank was purchased from Praxair and provided 300 ft^3 of regular air. The pressure regulator and related fittings that connected the air tank to the compressed air manifold were ordered from McMaster Carr and had a pressure range of 10 to 200 psi (1 psi = 6.89 kPa). The air manifold was ordered from McMaster Carr with a max flow rate of 20 scfm (note: 1 standard cubic feet of gas per minute (scfm) at 59 °F is equivalent to 0.00047 m^3/s) at 100 psi and a max pressure of 200 psi.

2.2. Materials

Tanks 1-3 had an inner square channel with an area approximately 4 in^2. Tank 4 was larger, roughly twice the cross-sectional area. A table salt (NaCl) was added to two of the tanks to allow for better bubble visibility as salt can reduce agglomeration of the bubbles, approximately 3 to 4.5 g. Tank 1 was run with just water using a 3/16" diameter copper tube. Tank 2 was run with a mixture of water and salt (NaCl) and 3/16" diameter copper tube. These two tanks were used for analyzing bubble flow. Tank 3 was run with also the mixture of water and salt (NaCl) and using a 3/8" diameter copper tube. This tank was used to analyze slug flow. Tank 4 was run with just water using a ½" diameter copper tube. As with tanks 1 and 2, this tank was used to explore bubbly flow.

2.2. Experimental Routines for Class Design

2.2.1. Pre-Class Procedure

The channel was filled with deionized water; however plain distilled water should be fine. Depending on the tank, the salt was added; for the proof of concept runs, this meant two of the tanks had salt and two were without. After the salt had dissolved into the water, the copper tube assembly was lowered into the tank and connected to the air supply. The flow meter was then set to the 0 units, the regulator valve was closed, and the air tank valve was opened. The regulator was slowly brought up to 45 psi and then the flow meter was brought to the desired flow rate.

For the pre class data recording, a flow rate of 2 square cubic foot per minute (scfm) was used. Video can be recorded at 960 frames per second (fps) for 10 seconds. After transfer to the computer, the video can be analyzed using the in-class procedure described below.

2.2.2. During Class Procedure

For Tanks 1 and 2, bubbly flow was recorded using a smart phone, either an iPhone or a Samsung phone. The video was to be recorded in 1080p HD at 240 fps in Slo-mo. The recordings were done for a maximum of 10 seconds. Videos were recorded until the bubbles were clearly seen and it was easy to identify a bubble to track. A sample of a useable video still is shown in Figure 2.4. Each assigned team can then adjusted the flow rate until the behavior described by Curve BC was seen (see the discussion in Chapter 1). Information gathered from this video was then recorded.

Figure 2.4: Sample image from a proper recording video.

For Tank 3, the teaching assistant in charge of the experiment can help demonstrating a plug flow for each team. The change in fluid height before the plug and at the highest point before plug collapse could be recorded. This information along with the area of the tank could be used to calculate the volume change.

For Tank 4, video of bubbly flow in the tank was recorded. The gas flow rate was increased at the team's discretion and information about that was recorded.

2.2.3. Video Analysis

As the recording software needed to analyze the video was on the lab computers, each team had to email themselves their selected videos. During this process, it was discovered that recording a video with an iPhone was the better option as it was compressed automatically when sent through the mail app. After the video was on the computer, each team could use VLC to turn the video into several still images. The process behind creating the stills in VLC is as follows. First, the students had to create a folder to store the frames and then copy the path to it (see Figure 2.5). Note: For Mac OSX/Linux users only, this must be the full path.
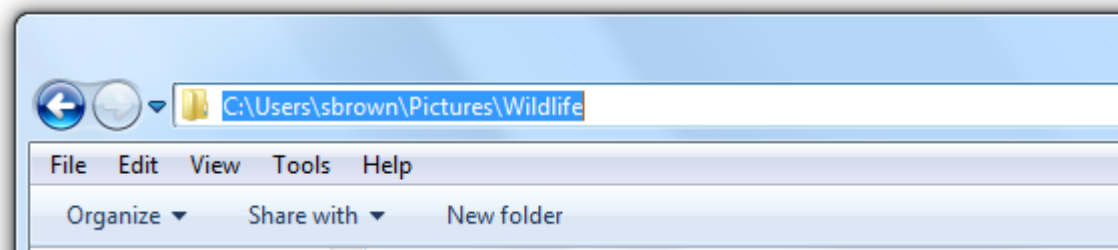
Figure 2.5: Video path

In the preferences menu, the all option was chosen under Show Settings. This enabled them to then select the required scene video filter and scene filter. They then pasted in the path to the chosen photo folder (see Figure 2.6). In order to get the best results, the recording ratio was set to 1. This would export each frame. The teams then saved the changes and opened the desired video. While playing, the teams would press Control+J to see the video information and then record the video frame rate. This information will be used for your frame rate. After the video ended, the Scene video filter was unchecked in order to prevent overwriting thumbnails in the current folder.
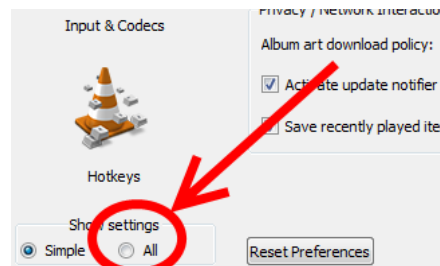
Figure 2.6: Settings menu

After those steps were done, the TA provided each team with ImageJ. Once installed, the directory of the generated images was imported. The Sequence Options will appear as shown in Figure 2.7.
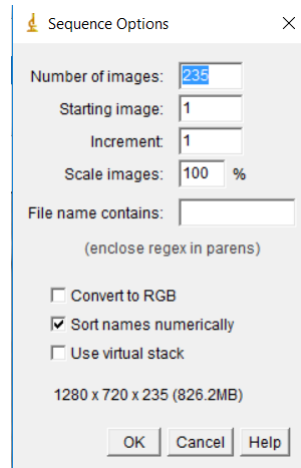
Figure 2.7: Sequence options menu

The sequence could be started approximately halfway through the total number of images in the folder. In order to ensure efficient processing, the max number of images was set to 60. Once the sequence was set, the pixel conversion to obtain the velocity was performed. First, the scale was determined using the tank markings and the pixel coordinates, shown in the Figure 2.8.
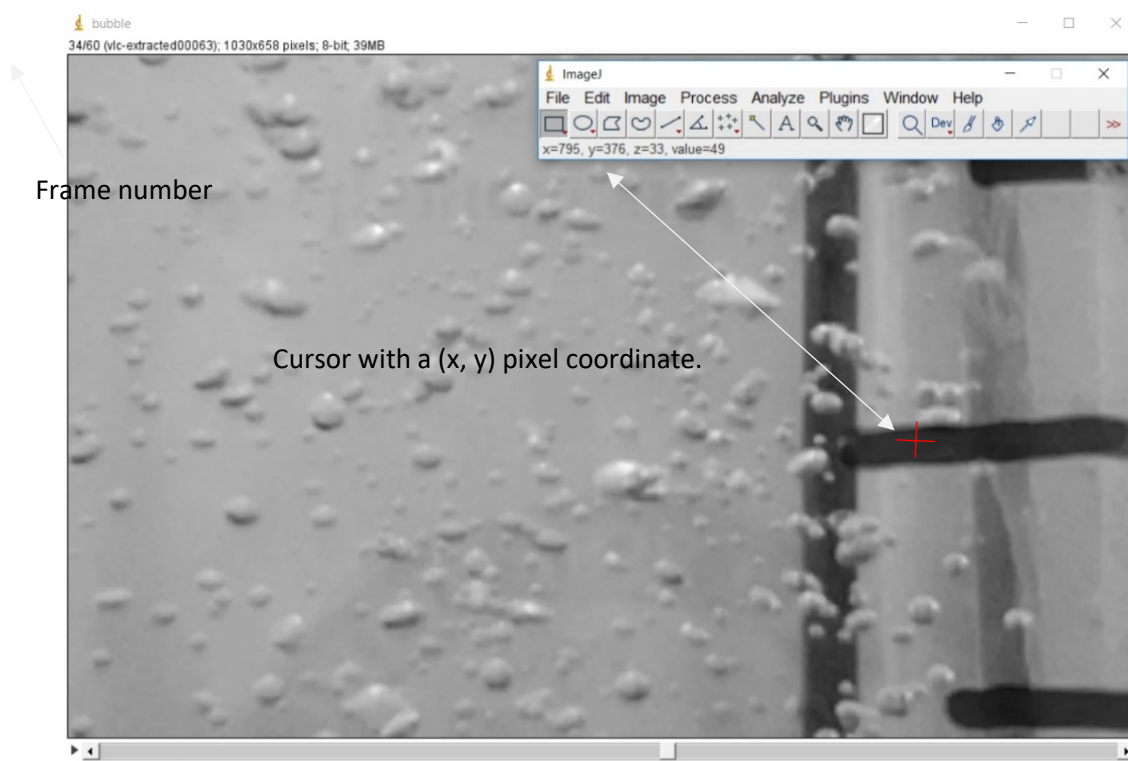
Figure 2.8: Pixel coordinates and frame number

This was done 3 to 5 times in order to get an average pixel per inch (ppi) value. After this value was obtained, the teams tracked a chosen bubble over a chosen number of frames. With the average ppi value and the frame rate, the teams then determined the bubble velocity. A flow chart of the recommended procedure is below, Figure 2.9.
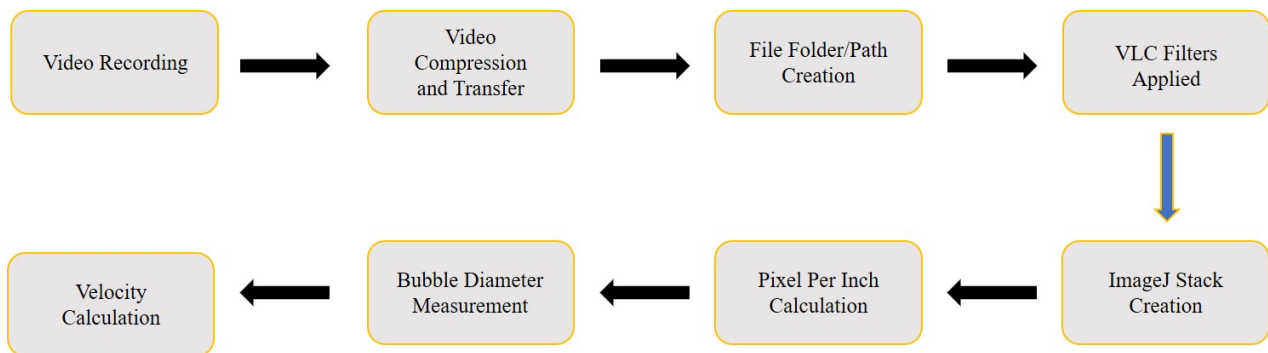
Figure 2.9: Video analysis flowchart

Chapter 3 Results and Discussion

The experiments provided evidence that there is an ability to simulate the flows described in Chapter 1. Bubbly, churn, slug, and plug flows were able to be produced. Volume changes produced by the slug and plug flows could be demonstrated adequately. Approximate flow velocity calculations were able to be done for the bubbly flows. The best takeaway was the photo quality. While cell phone cameras could take good still images, once the scene became chaotic, it got harder to take a high-quality image; so quality could have been compromised. This became very evident when trying to determine bubble population. However, since most of the calculations would be done live in a laboratory setting, the students would not experience these problems and could get more accurate height and bubble size values. Average bubble diameters and velocities were calculated for the two tanks demonstrating bubbly flow from data gathered in lab. Units were presented in mm and mm/s due to the overall size of the bubbles in the flows.

3.1. Different Flow Observations

3.1.1. Bubbly Flow

The tanks demonstrated the ability to produce bubbly flow, as shown in Figure 3.1. The results show that the bubbles in the flow are reasonably distributed throughout the tank. The bubble size distribution appears to be reasonable with few if any giant bubbles or slugs present.

Figure 3.1: Bubbly Flow (L and R), red lines indicate ½" (~12.7mm) increase in height

3.1.2. Bubbly Flow - Population

By applying a second filter when calculating bubble diameter, it was also possible to estimate bubble population. While the image quality reduces the validity and accuracy of these results by a considerable amount, note that it is possible that using a better camera will yield a more accurate result. Optionally, a different background behind the tanks could provide the contrast required and allow for better results without needing to change equipment. Figure 3.2 shows the difficulty in getting a precise count using the natural background present in Figure 3.1. This image shows the results of using the 12 preset threshold settings in ImageJ in order to separate the bubbles from the background.

Figure 3.2: Montage of Threshold results

From this montage, it was decided that the best option for bubble population calculation was to be the percentile threshold, shown in Figure 3.3 as the last image in row 3. Compare these images to the right image of Figure 3.1. The percentile threshold was modified to provide the clearest image of bubbles yet there are still large areas of black, which are not bubbles at all, they are background. Despite these impacts to the bubble population count, it is possible to get a rough

estimate. In this case, the bubble population was estimated to be 384 (see Figure 3.4). A better background or camera would reduce noise and thus improve this estimate.

Figure 3.3: Post threshold estimated bubble locations
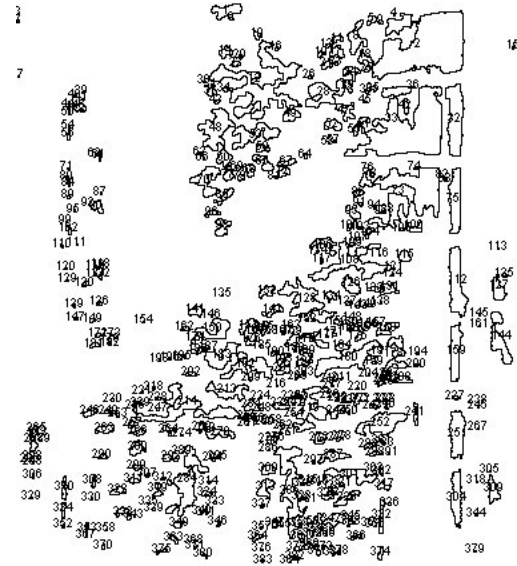
Figure 3.4: ImageJ estimate of bubble locations

3.1.3. Bubbly Flow - Velocity

The average velocity of the flow in Tanks 1 and 2 was calculated. This shows that it is possible to calculate bubble velocity; however, there are some issues. For tank 1, the average flow velocity was 195.9 ± 132.6 mm/s. For tank 2, it was 187.3 ± 104.1 mm/s. The standard deviations of the calculated velocities are extremely high. This is due to the large range of bubble velocities, with the minimum recorded and maximum recorded velocities shown in Table 3.1, with a plot of the overall velocities shown in Figure 3.5.

Table 3.1: Bubble Velocity (mm/s)

	Velocity (mm/s)	Standard Deviation (mm/s)	Max Velocity (mm/s)	Min Velocity (mm/s)
Tank 1	195.9	132.6	417.1	16.9
Tank 2	187.3	104.1	325.1	29.2

31
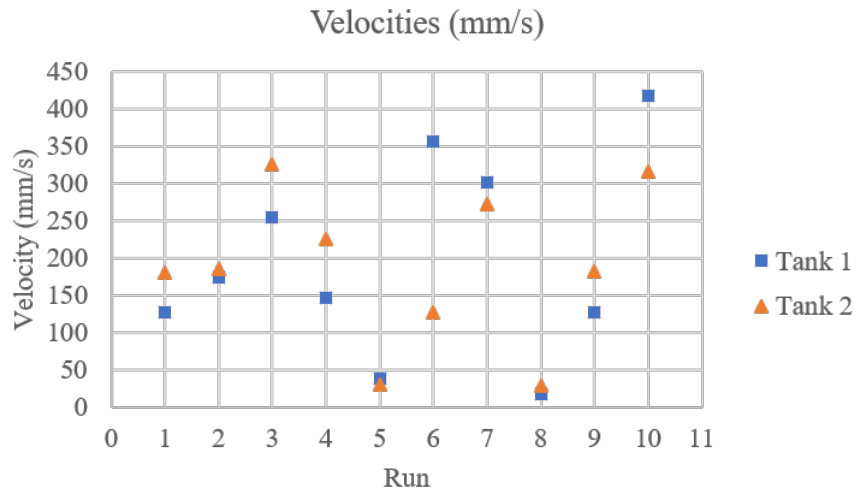
Figure 3.5: Velocities per run

The most probable reason the bubble velocities have such a broad range is due to the user. The air volumetric flow rate was to be set at 2 ft^3/h or roughly 0.0566 m^3/h however, in order to get flow that was clear to image, it may have been set higher or lower at the groups discretion. As seen in some of the figures, bubbles are not hard to spot but if care is not taken it might be hard to follow from frame to frame. A second, and also probable, reason would be the tracking method used. Bubbles were only followed in one direction, vertically (the y-axis). Any movement in any other direction was not taken into consideration and any effects that would have on the bubble velocity was thus not calculated.

3.1.4. Bubbly Flow - Average Diameter

The average diameter of group chosen bubbles in the flow in tanks 1 and 2 was calculated. This proves that it is possible to calculate bubble diameter using the method stated in the procedure. However, as with the velocity, there are some issues. For tank 1, the average bubble diameter was

32

3.52 ± 2.14 mm and in tank 2 the average bubble diameter was 4.29 ± 2.34 mm. The standard deviations of the calculated diameters are once again extremely high. The minimum recorded and maximum recorded velocities shown in Table 3.2. Figure 3.6 shows the average diameters at different runs.

Table 3.2: Bubble Diameter (mm)

	Diameter (mm)	Standard Deviation (mm)	Max Diameter (mm)	Min Diameter (mm)
Tank 1	3.52	2.14	7.11	0.94
Tank 2	4.29	2.34	10.2	1.73
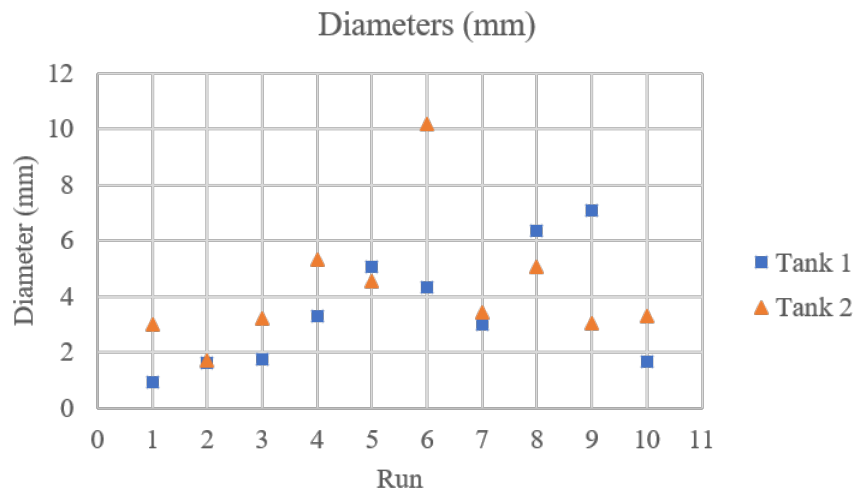
Figure 3.6: Diameters per run

3.1.5. Churn Flow

As the air flow rate increases into the tank, the less evenly distributed the bubbly flow became and churn flow started to appear. The difference in the bubble flows is clearly noticeable, shown in Figure 3.7. In this state, it is evident that it has become harder to isolate a bubble in the main flow and track it. The bubbles in this tank tended to stay in a centralized path away from the

walls until they reached an appropriate height from the source, approximately 5" from the top of the stone. This image was taken from video that was recorded at an air tank pressure of approximately 45 psi and a gas speed of 20 scfm.
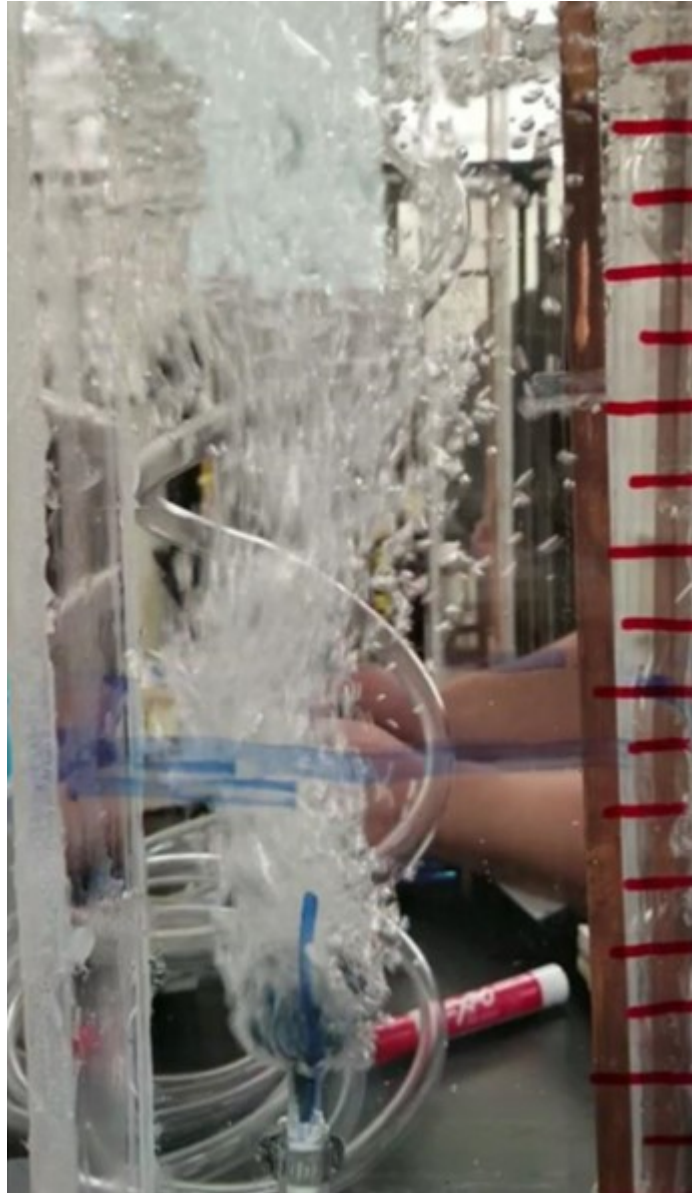
Figure 3.7: Churn flow

3.1.6. Slug Flow

The tanks were able to produce slugs. Each slug was produced by a sudden injection of air into the system. As these injections were done at the discretion of the operator, there is no data to

indicate the amount of air injected other than the calculations done by each group by calculating the volume change before the slug injection and after the slug has reached maximum height in the channel. The slug in this case was approximately 4.25" in height. Overall tank volume change was able to be measured by using height differences which are indicated by the arrows in Figures 3.8 and 3.9. As seen in Figure 3.9, the slugs were followed by churn flow. Unlike the churn flow shown in Figure 3.7, this flow behavior was not constant and dissipated quickly after the slug collapsed.
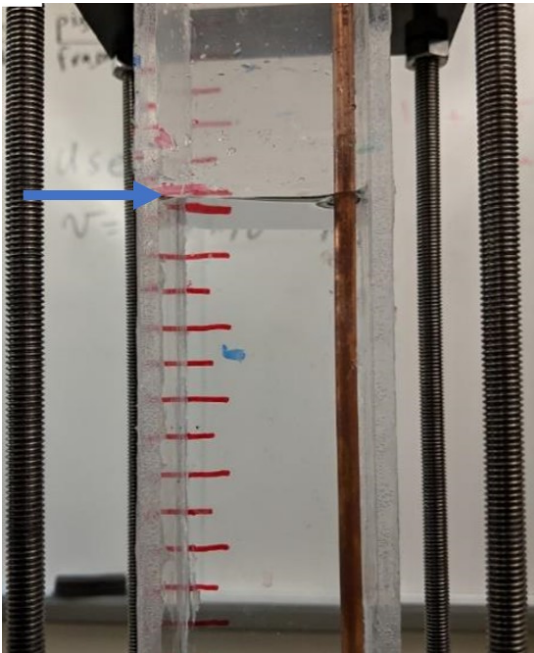
Figure 3.8: Water level before slug
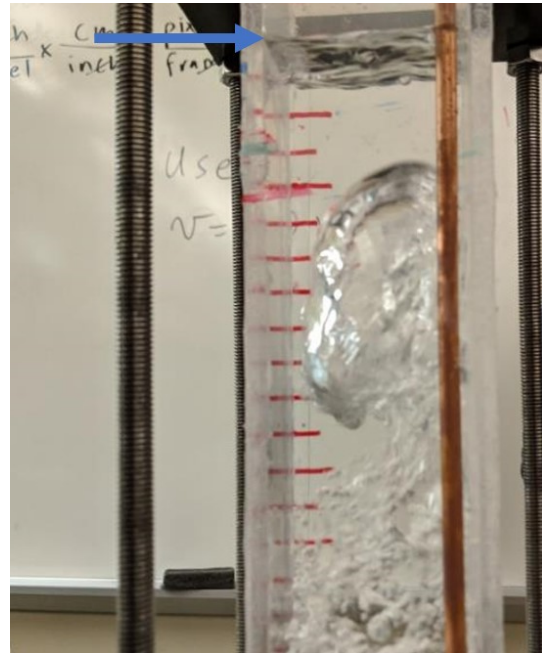
Figure 3.9: Water level during slug ascension

Shown in Figure 3.10, there are several features that can be identified. Point A shows the point where the flow was beginning to rotate around itself at the base of the slug. The areas identified as Points B are locations where the bubbles are no longer spherical, instead having oblong shapes. The bubbles identified at C are clearly no longer similar in size, unlike those in the bubbly flow.

35
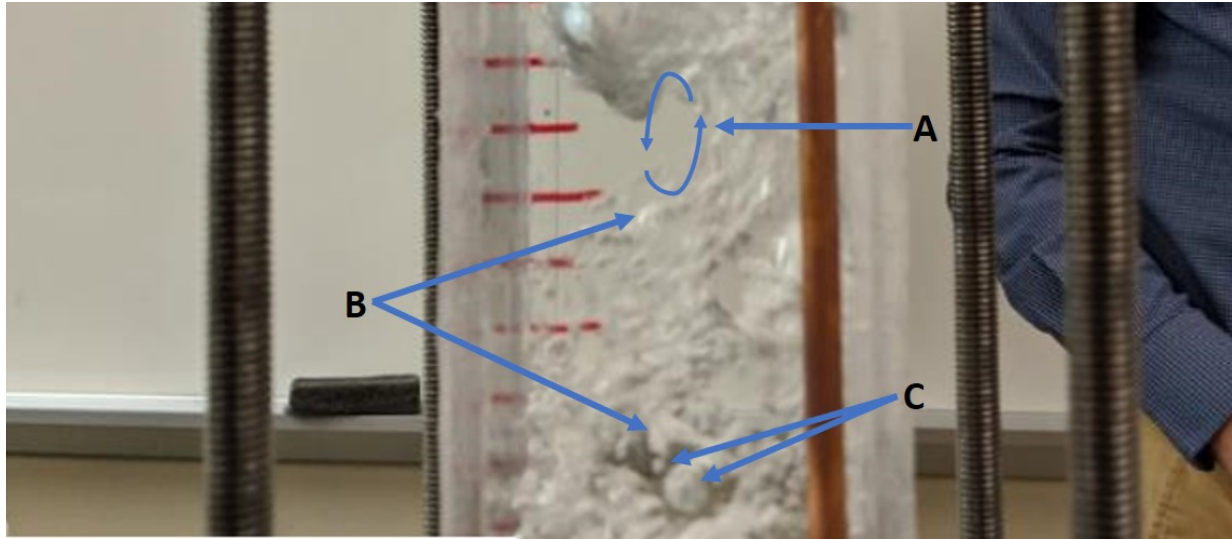
Figure 3.10: Observed churn characteristics. A. Area of Rotation; B. Elongated bubbles; C. Variable bubble size

3.1.7. Plug Flow

The tanks were able to produce plug flow, shown in Figure 3.11. The plugs are well defined. In the figure above, the plug is approximately 7" in height based on the half inch marks visible on the left-hand side. The plug is roughly the width of the tank at its base and slightly smaller at the top. As with the slugs, the plugs noticeably changed the total occupied volume inside the container. The red line indicates initial water height. Also similar to the slug flow, a rough volume change calculation can be obtained using the bubble height and the tank dimensions. The plug is followed by a churn flow, visible under the red line on the tank. This churn was due to the sudden injection of air into the tank. In this churn area, it is no longer possible to identify a single bubble for tracking.

Figure 3.11: Plug Flow

3.2. Summary

The results indicate that it is possible to adequately demonstrate bubbly, slug, plug and churn flow using the designed set up as well as photograph them using cell phone cameras. It is also possible to measure bubble velocities and diameters, as well as determine bubble population using the methods described. In the bubbly flow regime, for tank 1, the average flow velocity was 195.9 ± 132.6 mm/s. For tank 2, it was 187.3 ± 104.1 mm/s. For tank 1, the average bubble diameter was 3.52 ± 2.14 mm and in tank 2 the average bubble diameter was 4.29 ± 2.34 mm. The bubble

37

population in the 3.5" x 2.25" area shown in Figure 3.4 was measured to be 384 bubbles, though this estimate does not consider the bubble field depth nor does it consider errors from the chosen thresholding. Churn flow is present in multiple conditions: as a constant flow pattern when air is injected into the system at 45psi and 20scfm, as well as being a secondary flow pattern following the sudden injection of air to produce both slug and plug flows. In the slug and plug flow patterns, this churn flow dissipated upon the air pocket collapse. Both slug and plug flows were produced and volumes were easily able to be estimated using the water level pre-injection and the maximum displaced water height before the eventual pocket collapse, with plug flow water displacements as large as 7" being recorded. As mentioned, quality degradation resulting from video compression during transfer was an issue however it did not prevent adequate estimates from being made in any calculation. Fixes for this image quality issue as well as suggested ways to standardize the experiment will be discussed in Chapter 4.

Chapter 4 Summary and Future Plan

4.1. Summary

To verify the vertical bubble flow experiment, work had to take place in 3 phases. Phase 1 was the experimental design phase. Each tank was planned, manufactured and constructed. Once we check on the leaking status of each tank, we could continue with phase 2. During this phase, we explored the proof of concept in which the tanks were shown they would be able operate in the proposed design. Bubbly, slug, churn and plug flow patterns were all tested. Once satisfied with the results of phase 2, we started with phase 3, where we tested the experiment in a classroom setting. Each tank was set up and then the experiments were performed by approximately 30 - 40 groups (each group composed of 4 - 5 students).

As shown in the Results section (Chapter 3), it is possible to demonstrate the multiple flow patterns mentioned in the introduction. Using the *ImageJ* tracking method, the students were able to identify and follow a bubble along its rise in a water tank. Using this tool, it was possible for all students to calculate bubble velocity and bubble diameter.

4.2. Plan for Improvement - Manufacture

There were several problem areas that became apparent during the manufacturing process of the tanks, most importantly:

1. Cutting - During the process of gluing the tanks, it was found that not all the pieces were cut straight. This led to gaps during assembly.

2. Gluing - When gluing the tank pieces together, the Plexiglas was not properly covered to avoid excess adhesive from getting all over the material. There was underestimation in the

amount of adhesive needed both before and during construction. This led to scraping of the glue after drying which led to compromising visibility through the tank.

3. <u>Tank Marking</u> - Each tank was marked off at the half inch; however, this was done on one edge as opposed to going across the entire side of the box. This is a minor issue but it made recording and measuring a little more challenge.

To improve upon these issues, the following steps are recommended. For ensuring the boxes are the correct dimensions, if possible, have a single person oversee cutting the materials. Having to get the Plexiglas and other parts cut by two different technicians led to an issue in the cuts which could be remedied by getting everything together at once and then submitting an order. Alternatively, having the plastic cut in house could prevent that step all together assuming the necessary tools are available.

During the gluing process, properly covering the material that needs to be left clean must be done. This will eliminate the need for post drying scraping while ensuring only the edges that need to be connected are glued. The reduced scraping will provide for better visibility in the final product. This should also aid in reducing the amount of adhesive used and therefore reduce the amount needed overall.

The tank markings should be stretched across the whole of the side of the tank, if not wrap around the entire vessel. This would allow for recording from any angle as well as both x- and y-axis tracking of bubbles assuming that is required. Additionally, the tank marking across the entire tank would, in theory, keep the entirety of the line and prevent the line edge from raising or dipping.

4.3. Plan for Improvement - Standardization

There were also issues with the standardization of post construction processes; these important concerns including:

1. <u>Camera</u> - Having different phone cameras with different recording frame rates and different definitions caused issues. Videos recorded on Samsung phones would not properly compress and would not work when using ImageJ. The video sent to an iPhone would compress but in doing so would automatically change the frame rate without making the student or operator aware.

2. <u>Camera Stands</u> - The stands used were adequate but with the size of current phones make it difficult to get them to stay in place while trying to film the side of the tank with the markings.

To improve upon these issues, the following ideas are recommended. If possible, require each group to have an iPhone user. This would allow for setting specific FPS and definition requirements that would in turn allow each group to be working with the same initial information. Secondly, doing this option gives each group the ability to have the video recorded and compressed by the same person, which is a huge benefit. These steps, along with keeping the Plexiglas clean as previously mentioned, would allow for better overall video quality and allow for better tracking of the target bubble per group. Each group having the same FPS and definition requirements would then provide a way to fix issues that occur during the video processing part of the experiment.

A better way to direct the cameras at the target area should be created. This could be made in house the same way the tanks are. Each group having the same fixed height stand would also help with tracking, as they would, in theory, all be shooting the same area of the tank; therefore, they would have a similar experience in tracking their bubbles/ viewing the flows. This would also

allow for a standard background to be used. By fixing the area of interest, it would be possible to darken the target area which allow for better focused images. This improved focus would allow for better tracking for velocity as well as determination of diameter and bubble populations. It is important to note that there are phone stands that are adequate in case another way cannot be found and perhaps with the increase in visibility due to the manufacture improvements may be all that is necessary. The issue with these stands, however, is that they would need to be carefully set up and measured by whoever is in charge of the experiment before any flows can be observed in an effort to keep each group's recordings in the same location.

4.4. Suggestions

A suggestion for the experiment would be to replace the air tank with submersible heating elements. There are multiple downsides to this suggestion. The tanks would need suitable time to cool down between groups otherwise the boiling behavior would be more difficult to observe. Along the same line, the materials the tanks are being constructed of would need to be able to handle boiling water. Additionally, there is an inherent safety issue when working with electronics and water so each experiment would have to be handled by the professor or TA running the session, but if the element is rated submersible, this should not pose too big an issue. Another downside is cost, as buying four elements would likely cost more than buying one air tank.

There are also multiple upsides to this modification. First, the experiment would more closely resemble the behavior of the fuel rods in a reactor and allow the students to see the different boiling phases. The overall set up would be smaller which would help offset some of the cost of the heating elements. Each tank would be shorter and narrower thus needing smaller supports and a smaller base. This suggestion would also allow for a cleaner way to have multiple tanks, with

each tank having its own element as opposed to each tank being connected to the same air supply

via a tangle of hoses and connectors.

Chapter 5 References

[1] "Nuclear Fuel and its Fabrication." *Nuclear Fuel Fabrication - World Nuclear Association*, www.world-nuclear.org/information-library/nuclear-fuel-cycle/conversion-enrichment-and-fabrication/fuel-fabrication.aspx.

[2] Spinrad, Bernard I., and Wade Marcum. "Thermal, Intermediate, and Fast Reactors." *Encyclopædia Britannica*, Encyclopædia Britannica, Inc., 5 Sept. 2019, www.britannica.com/technology/nuclear-reactor/Thermal-intermediate-and-fast-reactors#ref45768.

[3] "Nuclear Power Reactors." *Nuclear Reactors | Nuclear Power Plant | Nuclear Reactor Technology - World Nuclear Association*, 2020, www.world-nuclear.org/information-library/nuclear-fuel-cycle/nuclear-power-reactors/nuclear-power-reactors.aspx.

[4] "Pool Boiling – Boiling Curve." *Nuclear Power*, www.nuclear-power.net/nuclear-engineering/heat-transfer/boiling-and-condensation/pool-boiling-boiling-curve/.

[5] Todreas, Neil E., and Kazimi, Mujid S. *Nuclear Systems Vol. 1: Thermal Hydraulic Fundamentals*. 2nd edition. CRC Press: Taylor & Francis Group, 2011, pp. 603 – 607.

[6] Usui, Kensuke, and Kazuo Sato. "Vertically Downward Two-Phase Flow, (I)." *Journal of Nuclear Science and Technology*, vol. 26, no. 7, 1989, pp. 670–680., doi:10.1080/18811248.1989.9734366.